RSC Advances

ROYAL SOCIETY OF CHEMISTRY

www.rsc.org/advances

Simultaneous determination of the cytokeratin 19 fragment and carcinoembryonic antigen in human serum by magnetic nanoparticle-based dual-label time-resolved fluoroimmunoassay

Guanfeng Lin[a†], Hui Zhao[b†], Tiancai Liu[a], Jingyuan Hou[a], Zhiqi Ren[a], Wenhua Huang[b], Wenqi Dong[c] and Yingsong Wu[a,] *

[a]Institute of Antibody Engineering, School of Biotechnology, Southern Medical University, Guangzhou, China.

[b]Department of Human Anatomy, School of Basic Medical sciences, Southern Medical University, Guangzhou, China.

[c]Department of Biopharmaceutical, School of Biotechnology, Southern Medical University, Guangzhou, China.

*Corresponding author, wg@smu.edu.cn; Tel: +86-20-62789355; Fax: +86-20-37247604.

[†] Contributed equally

Abstract

A highly sensitive, rapid and novel simultaneous measurement method for cytokeratin 19 fragment (CYFRA 21-1) and carcinoembryonic antigen (CEA) in human serum by magnetic nanoparticle-based dual-label time-resolved fluoroimmunoassay was developed. Based on a sandwich-type immunoassay format, analytes in samples were captured by antibodies coating onto the surface of magnetic beads and sandwiched by other antibodies labeled with europium and samarium chelates. The lower limit of quantitation of the present method for CYFRA 21-1 was 0.77 ng/ml and CEA was 0.85 ng/ml. The coefficient variations of the method were less than 7%, and the recoveries were in the range of 90-110% for serum samples. The concentrations of CYFRA 21-1 and CEA serum samples determined by the present method were compared with those obtained by the chemiluminescence immunoassay. A good correlation was obtained with the correlation coefficients of 0.961 for CYFRA 21-1 and 0.938 for CEA. This novel method demonstrated high sensitivity, wider effective detection range and excellent reproducibility for simultaneous determination of CYFRA 21-1 and CEA can be useful for early screening and prognosis evaluation of patients with lung cancer.

Keywords: Magnetic nanoparticle; Dual-label time-resolved fluoroimmunoassay; Cytokeratin 19 fragment; Carcinoembryonic antigen

Abbreviations

NSCLC, non-small cell lung cancer; **CYFRA 21-1**, Cytokeratin 19 fragment; **CEA**, Carcinoembryonic antigen; **TRFIA**, time-resolved fluoroimmunoassay; **CLIA**, chemiluminescence immunoassay; **Eu**, europium; **Sm** samarium; **Tb**, terbium; **McAb**, monoclonal antibody; **LLOQ**, lower limit of quantitation; **RE**, relative error; **CV**, coefficient of variation; **SD**, standard deviation; **BSA**, ovine serum albumin; **MES**, 4-morpholineethanesulfonic

acid; **NHS**, n-hydroxysulfosuccinimide; **EDC**, 1-ethyl-3-(3-dimethylaminopropyl) carbodiimide hydrochloride

Instruction

Lung cancer is the most prevalent and generally has a very poor prognosis worldwide, and non-small cell lung cancer (NSCLC) accounted for about 85% of lung cancer cases [1, 2]. By improving prognosis, early diagnosis is paramount to improve the survival of lung cancer patients at present [3, 4]. Additionally, accurate and effective prognosis evaluation of lung cancer is also a mainstay for improving the survival of lung cancer patients. In clinical, diagnostic methods usually used for lung cancer include computed tomography, bronchoscopy and sputum analysis, which all have limitations for early diagnosis of lung cancer [5]. Thus, it appears that a more efficient detection method such as using serum tumor markers may complement those diagnostic methods in the early diagnosis of lung cancer [6].

Serum tumor markers are non-invasive diagnostic tools for identifying malignant tumors, and are commonly used for the early screening of cancer and as an indicator of treatment efficacy. Cytokeratin 19 fragment (CYFRA 21-1) is a cytokeratin expressed in simple epithelium, including the bronchial epithelium, and in malignant tumor derived from these cells. CYFRA 21-1 is the most sensitive tumor marker for NSCLC, particularly squamous cell tumors [7]. Carcinoembryonic antigen (CEA) is an oncofetal glycoprotein of the cell surfaces. In small quantities it is present in cells of normal tissues in healthy adults. CEA concentrations are particularly high in adenocarcinoma and large cell lung cancer, but the elevated concentrations also found in various benign pathologies and other malignancies preclude its use in screening and limit its diagnostic use. However, CEA may be helpful in the differential diagnosis of non-small cell lung cancer, preferably in combination with CYFRA 21-1 [8-11]. A number of immunoassay methods for CYFRA 21-1 and CEA have been reported [12-17]. However, CYFRA 21-1 and CEA never be detected simultaneously in the currently available methods. Time-resolved fluoroimmunoassay (TRFIA)

using lanthanide complexes chelates as the labels was used as an 'ideal' immunoassay method when it was first reported by Lovgren et al [18]. Time-resolved fluorometry of lanthanide chelates has been shown to be one of the most successful non-isotopic detection techniques, and dual-label TRFIA has been employed in numerous applications in the biomedical sciences [19-25]. We first reported the application of magnetic nanoparticle in TRFIA [13]. The combination of TRFIA and magnetic nanoparticle improves sensitivity and significantly reduces the analysis time via a homogenous format, and provides an interesting alternative tool for the determination of serum tumor markers in clinical laboratories [13, 26]. As a highly sensitive method and employed in numerous applications for simultaneous determination of multiple analytes, magnetic nanoparticle-based dual-label TRFIA will certainly lead the innovation of detection method. We innovatively developed a magnetic nanoparticle-based dual-label TRFIA, which was designed specifically as a sensitive, precise and rapid measurement method for the early screening and prognosis evaluation of patients with lung cancer. Thus, the purpose of the present study was to develop a novel magnetic nanoparticle-based dual-label TRFIA and test its application for the simultaneous determination of CYFRA 21-1 and CEA in human serum. This study involved measurement of parameters, such as repeatability, recovery, linearity and feasibility.

Methods

Reagents and instrumentation

Bovine serum albumin (BSA), 4-morpholineethanesulfonic acid (MES), N-hydroxysulfosuccinimide (NHS), 1-ethyl-3-(3-dimethylaminopropyl) carbodiimide hydrochloride (EDC), proclin-300 and Tween-20 were purchased from Sigma-Aldrich (St. Louis, MO, USA). Sephadex G-50 was purchased from Amersham Pharmacia Biotech (Piscataway, NJ,

USA). All other chemicals used were of analytical reagent grade and ultra-pure water obtained using a Milli-Q water purification system (Millipore, MA, USA) was used throughout the experiments. Anti-CEA monoclonal antibodies (McAbs) (clone 5909 and 5910) and CEA antigen were purchased from Medix (Grankulla, Finland). Anti-CYFRA 21-1 McAbs (clone 1602 and 1605) were also obtained from Medix (Grankulla, Finland). CYFRA 21-1 antigen was purchased from BioDesign (Memphis, TN). Magnetic nanoparticle (1101GA-03) were obtained from JSR Life Sciences (Tokyo, Japan). A Victor^3 1420 Multi-label Counter for spectral analysis of fluorescent chelates, europium (Eu) and samarium (Sm) labeled kits were purchased from PerkinElmer Life and Analytical Sciences (Waltham, MA, USA).

Buffer solutions used in the study were coating buffer (0.1 mol/L MES, pH 5.0), labeling buffer (50 mmol/L Na_2CO_3-$NaHCO_3$, containing 0.9% NaCl, pH 9.0), assay buffer (25 mmol/LTris-HCl, containing 0.02% BSA, 0.09% NaCl, 0.05% Tween-20 and 0.05% proclin-300, pH 7.8), elution buffer (50 mmol/L Tris-HCl, containing 0.9% NaCl and 0.05% proclin-300, pH 7.8), washing buffer (50 mmol/L Tris-HCl, containing 0.9% NaCl, 0.2% Tween-20 and 0.05% proclin-300, pH 7.8), standard buffer (50 mmol/L Tris-HCl, 0.2% BSA and 0.1% NaN_3, pH 7.8), blocking buffer (5% BSA, pH 7.0) and enhancement solution (100 mmol/L acetate-phthalate,0.1% triton X-100, 15 μmol/L β-naphthoyltrifluoroacetate, 50 μmol/L tri-*n*-octylphosphine oxide, pH 3.2).

Coating conjugate preparation

Covalent conjugation between magnetic nanoparticle and anti-CYFRA 21-1 McAb (clone 1602) was carried out as described in our previous work. Briefly, 500 μL of magnetic nanoparticle (20 mg/mL, 2.0×10^9 magnetic nanoparticle/mL in H_2O) was suspended in 500 μL coating buffer.

Then, 25 μL of EDC (10 mg/mL) and 40 μL of NHS (10 mg/mL) freshly prepared were added into the above magnetic nanoparticle suspension and the resultant mixtures were incubated at room temperature under gentle stirring to activate the carboxylic acid groups on the surface of the magnetic nanoparticle. After incubation for 30 min, the activated magnetic nanoparticle were magnetically isolated, followed by rinsing with coating buffer three times. Subsequently, 100 μg anti-CYFRA 21-1 McAb (clone 1602) was added to the activated magnetic nanoparticle in 1 mL coating buffer. The reaction proceeded at room temperature for 18 h under gentle stirring and the mixtures were subsequently rinsed four times with assay buffer to remove unbound antibody using magnetic separation. The resultant magnetic nanoparticle were resuspended in 1 mL blocking buffer at room temperature for another 3 h to eliminate nonspecific binding effects and block the remaining active groups. After a final rinsing with assay buffer, the magnetic nanoparticle–antibody conjugates were resuspended in assay buffer and stored at 4 °C until use. The anti-CEA McAb (clone 5910) was conjugated to magnetic nanoparticle using a similar method.

Antibody labeling

Anti-CEA McAb (clone 5909) and anti-CYFRA 21-1 McAb (clone 1605) were labeled with Sm^{3+}- and Eu^{3+}-chelates using the labeling buffer, respectively. Initially, 1mg anti-CEA McAb (clone 5909) was gently mixed in 200 μL of labeling buffer with 500 μg of Sm^{3+}-chelates in 100 μL of the same buffer. After an 18 h incubation with continuous gently shaking at room temperature, free Sm^{3+}-chelates and aggregated McAb were separated from Sm^{3+}-McAb conjugates using a 1 cm × 40 cm column packed with sepharose CL-6B (lower 20 cm), eluted with a descending elution buffer, and collected with 1.0 mL per fraction. The concentration of

Sm^{3+}-conjugates in collected fraction was measured with fluorescence, and diluted with an enhancement solution (1:1000). The fluorescence in microtitration wells (200 μL per well) was detected by comparing the signal of samples to that of stock standards diluted at 1:100 in an enhancement solution. The fractions from the first peak with the highest Sm^{3+} count were pooled and characterized. Eu^{3+}-labeled anti-CYFRA 21-1 McAb (clone 1605) was prepared similarly. The labeled McAb was rapidly lyophilized under high vacuum after dilution with the elution buffer containing 0.2% BSA as a stabilizer, and stored at -20 °C. No loss of immunoreactivity was observed during a 6-mo storage period.

Preparation of CYFRA 21-1 and CEA standards

The concentrations of CYFRA 21-1 and CEA in the six mixed standards were prepared by diluting highly purified CYFRA 21-1 and CEA antigen in standard buffer both as 0, 5, 10, 50, 100 and 500 ng/mL.

Samples and comparison method

All samples were kindly provided by Nanfang Hospital (Guangzhou, China) with the CYFRA 21-1 and CEA values measured by chemiluminescence immunoassay (CLIA) (Abbott, IL, USA). All the patients were diagnosed on the basis of characteristic clinical features and confirmed by laboratory tests. These samples were stored at -20 °C. The collection and storage of the serum samples were carried out in accordance with The Code of Ethics of the World Medical Association (Declaration of Helsinki).

Assay protocol

The proposed immunoassay for the simultaneous quantitation of CYFRA 21-1 and CEA was performed based on a sandwich type immunoassay format by combining a TRFIA assay and

immunomagnetic separation, and was shown schematically in Fig. 1. Initially, 30 μL of standards or samples were added to each well, then 50 μL of magnetic nanoparticle coated with anti-CYFRA 21-1 McAb and 50 μL of magnetic nanoparticle coated with anti-CEA McAb were added, followed by the addition of 70 μL of assay buffer containing 300 ng Eu^{3+}-labeled anti-CYFRA 21-1 McAb and 700 ng Sm^{3+}-labeled anti-CEA McAb. The mixtures were subsequently incubated at room temperature for 45 min with continuous gentle stirring. Subsequently, the formed sandwich immunocomplexes were drawn to bottom of the test wells and separated from free substances by the application of a samarium–cobalt magnet. After removing the free substances and rinsing with washing buffer four times, 200 μL of enhancement solution was added and then the immunocomplexes were resuspended in enhancement solution and the mixtures were incubated for 5 min at room temperature with stirring. Finally, the fluorescence signal was measured using a $Victor^3$ 1420 Multi-label Counter (the mode of europium and samarium dual-label). The fluorescence of Eu^{3+} was measured at an excitation wavelength of 340 nm and an emission wavelength of 615 nm. The fluorescence of Sm^{3+} was measured at an excitation wavelength of 340 nm and an emission wavelength of 642 nm.

Validation experiment

Preliminary estimates of the lower limit of quantitation (LLOQ) were determined by identifying the lowest concentrations, for which the two-sided 90% SFSTP (Societe Francaise Sciences et Techniques Pharmaceutiques) confidence limits for percent relative error (RE) were within 25% of the nominal value as described by Findlay et al [27]. We spiked standard buffer with purified CYFRA 21-1 and CEA to obtain 7 preparations with final concentrations from 0.2 to 25 ng/mL. Each preparation was aliquoted (n=20) and stored at -70 °C. An aliquot of each

preparation was thawed and analyzed each day. This procedure was repeated in 20 independent assays on different days. The bias was defined as the difference between the overall mean of the measurements ($\bar{X}$) and the nominal value (Z). Estimated variance of $\bar{X}$ ($S_{\bar{x}}$) was determined by between-run ANOVA mean square errors. RE (%) including both bias and imprecision was estimated with the equation: $RE = (100/Z) \cdot [(\bar{X} - Z) \pm t_{0.10/2,\upsilon} \cdot S_{\bar{x}}]$, and the LLOQ was defined as the concentration where RE is 25% [28, 29]. Dilution linearity of assay was determined using serial dilutions from 2-fold to 16-fold with standard buffer for serum samples. High-dose signal saturation was performed in the range from 5 to 2000 ng/mL for CYFRA 21-1 and CEA. The analytical recovery was studied by adding purified CYFRA 21-1 and CEA antigen to serum samples. Serum samples were measured using the same batch of reagents on separate days for the evaluation of precision.

Statistical analyses

Analysis of data was performed using SPSS 13.0 (Chicago, IL, USA). Standard curves were obtained by plotting the fluorescence intensity (Y) against the logarithm of the sample concentration (X) and fitted to a four-parameter logistic equation using Origin7.5 SR1 (Microcal, USA): $LogY = A + B \times LogX$.

Results

Standard curve, signal saturation and lower limit of quantitation of the assay

A standard curve for the immunoassay was carried out following our protocol with a series of dilution of standards (0, 5, 10, 50, 100 and 500 ng/mL) obtained from 10 separate assays. Standard curve determinations were carried out using linear regression and log-log regression. For the standard curve depicted in Fig. 2, the best-fit calibration of CYFRA 21-1 was determined to be

described by the following equation: $\mathrm{LogY} = 3.17 + 1.02 \times \mathrm{LogX}$ (r^2=0.996, P<0.0001). For CEA, the equation was $\mathrm{LogY} = 2.46 + 1.00 \times \mathrm{LogX}$ (r^2=0.996, P<0.0001). Signal saturation ("hook" effect) were seen when the range exceeded 1000 ng/mL for CYFRA 21-1, and 500 ng/ml for CEA (Fig. 3). Within-assay coefficients of variation (n=10) using standards were less than 10% in the range. Graphical estimation indicates the lower limit of quantitation of the present method for CYFRA 21-1 was 0.77 ng/ml and CEA was 0.85 ng/ml (Fig. 4).

Analytical recovery

The analytical recovery was studied by adding purified CYFRA 21-1 and CEA antigen to 3 serum samples from different patients. The results were given in Table 1. The recoveries of added analytes were in the range of 90-110%.

Precision

Within-and between-assay imprecision were determined using three serum samples and the same batch of reagents on separate days as showed in Table 2. Total imprecision of the present TRFIA assay were ranged from 3.9% to 6.9% for CYFRA 21-1, and form 2.5% to 6.5% for CEA. As expected, the imprecision of the present TRFIA was remarkably low.

Dilution

Table 3 gives the results of our evaluation of the dilution linearity of this dual-label TRFIA when we used samples serially diluted with assay buffer. Expected values were derived from initial concentrations of analytes in the undiluted samples. Correlating the results obtained from dual-label TRFIA with the expected concentrations, we found that the dilution curves were linear over the whole range of concentrations. Expected and measured values were well correlated.

Comparison with CLIA

CYFRA 21-1 in 90 and CEA in 78 clinical samples were analyzed by the present TRFIA. The correlation of the CYFRA 21-1 values obtained by this method and those obtained by CLIA was excellent; the regression equation was $Y = 1.14 \times X - 1.60$ (r^2 =0.994, P<0.0001). For CEA, the regression equation was $Y = 0.28 + 1.00 \times X$ (r^2= 0.938, P<0.0001). The comparisons of CYFRA 21-1 and CEA values obtained by the two methods (TRFIA and CLIA) were shown in Fig. 5.

Discussion

Dual-label has potential applications in various fields. However, conventional fluorescent labeling has a limited success in the assay of multiple analytes, which makes it difficult to distinguish between the emission bands of the labellings [30, 31]. On the face of it, the use of lanthanide chelates seems the perfect solution. Because of the higher fluorescence yield and lower background, Eu^{3+} chelate is the most frequently used label in TRFIA. Terbium (Tb) chelate usually has a longer decay time and a higher fluorescence yield than Sm^{3+} chelate, and its fluorescence is less sensitive to aqueous quenching. Tb^{3+} chelate required an aliphatic β-diketone to enhance the fluorescence of Tb^{3+} [32]. Moreover, Eu^{3+} and Sm^{3+} chelates can use the same enhancement solution in immunoassay for multiple analytes. Combining the above factors, Eu^{3+} and Sm^{3+} chelates was selected as labels in our study.

With the rapid development of clinical diagnosis, the combined applications of serum tumor markers have been paid more and more attention by the researchers. To our knowledge, this work, which represented the first report of a dual-label CYFRA 21-1/CEA assay, demonstrates in principle, the feasibility of developing a multiplex assay for screening samples for multiple analytes in clinical diagnosis. However, a limitation is the Sm photoluminescence yield is much

lower than that of Eu, as Sm^{3+} is usually used as a tracer in assays not requiring a great sensitivity. And that is the reason why magnetic nanoparticle are applied in TRFIA. Magnetic nanoparticle as nanometer materials have been successfully employed in many areas of research, including cell separation, biomolecule detection, DNA extraction and various immunoassay methodologies [33-36]. Utilizing magnetic nanoparticle-beads could be a key to protect the specific antigen or antibody from being washed away. The magnetic nanoparticle-beads suspended in the reaction solution provided a relatively larger surface area. This enabled more antibodies to be coupled to the surface, thereby reducing the consumption of reagents and improving the immobilization of more antibodies. This led to appreciable improving of the sensitivity and precision for detection. With the help of magnetic nanoparticle-beads, the lower limit of quantitation of CEA in this novel dual-label assay was 0.85 ng/mL, whereas that of single Eu^{3+}-label assay was 0.5 ng/mL [13]. Despite this, the detection sensitivity for CEA with a lower limit of quantitation of 0.85 ng/mL can be more than adequate for determination of the CEA concentration in clinical samples.

Standard curves for CYFRA 21-1 and CEA showed excellent performance of our detection system. Average recovery rates for CYFRA 21-1 and CEA were in the range of 90-110%, respectively. Signal saturation were seen when the range exceeded 1000 ng/mL for CYFRA 21-1, and 500 ng/ml for CEA. Samples with three different concentrations of CYFRA 21-1 and CEA were analyzed at various dilutions, respectively. The percentage of expected values for CYFRA 21-1 and CEA were in the range of 90-110%, respectively. In addition, 30 μL of sample was enough for the simultaneous detection of CYFRA 21-1 and CEA. Those all showed that this magnetic nanoparticle-based dual-label assay was satisfactory for clinical use. Dual-label TRFIA can measure the concentration of CYFRA 21-1 and CEA, as well as the ratio of CYFRA

21-1/CEA. Thus reducing the random handling errors and increasing the clinical confidence level of CYFRA 21-1/CEA ratio. Direct labeling of immune reagents with lanthanide chelates and lack of overlapping between Eu^{3+} and Sm^{3+} chelates allow a rapid assay. Additionally, antibody-coated magnetic nanoparticle-beads employed as a solid phase in suspension to capture analytes enabled more antigens to become accessible within a short time. Hence, antigen-antibody equilibrium could be achieved more rapidly, which further reduced the analysis time.

Conclusions

In summary, we have developed a novel magnetic nanoparticle-based dual-label TRFIA, which was designed specifically as a hypersensitive, precise and rapid measurement method for simultaneous determination of the CYFRA 21-1 and CEA in human serum. The present method established here, when applied to the determination of CYFRA 21-1 and CEA in human serum, showed excellent correlation with the conventional CLIA. Additionally, this novel method demonstrated high sensitivity, wider effective detection range and excellent reproducibility for the determination of CYFRA 21-1 and CEA, and offered the additional benefit of faster detection, resulting in a substantially faster assay. Our novel assay can be useful for early screening and prognosis evaluation of patients with lung cancer by minimizing time, lowering sample consumption and increasing accuracy. Based on this investigation, we established a good foundation for further development of other biomarkers using the same platform.

Competing interests

The authors declare that they have no competing interests.

Acknowledgements

The work was supported by the National Natural Science Foundation of China (Grant No.

81271931) and the Natural Science Foundation of Guangdong Province (Grant No. S2012010009547).

References

1. T. Hanagiri, M. Sugaya, M. Takenaka, S. Oka, T. Baba, Y. Shigematsu, Y. Nagata, H. Shimokawa, H. Uramoto, M. Takenoyama, K. Yasumoto and F. Tanaka, *Lung Cancer*, 2011, **74**, 112-117.
2. A. Jemal, R. Siegel, E. Ward, Y. Hao, J. Xu and M. J. Thun, *CA Cancer J Clin*, 2009, **59**, 225-249.
3. T. Hanagiri, T. Baba, T. So, M. Yasuda, M. Sugaya, K. Ono, T. So, H. Uramoto, M. Takenoyama and K. Yasumoto, *J Thorac Oncol*, 2010, **5**, 825-829.
4. J. H. Schiller, *Oncology*, 2001, **61 Suppl 1**, 3-13.
5. J. Hur, H. J. Lee, J. E. Nam, Y. J. Kim, Y. J. Hong, H. Y. Kim, S. K. Kim, J. Chang, J. H. Kim, K. Y. Chung, H. S. Lee and B. W. Choi, *BMC Cancer*, 2012, **12**, 392.
6. J. L. Mulshine and D. C. Sullivan, *N Engl J Med*, 2005, **352**, 2714-2720.
7. P. Wang, Y. Piao, X. Zhang, W. Li and X. Hao, *Cancer Biomark*, 2013, **13**, 123-130.
8. V. Barak, H. Goike, K. W. Panaretakis and R. Einarsson, *Clin Biochem*, 2004, **37**, 529-540.
9. J. Bates, R. Rutherford, M. Divilly, J. Finn, H. Grimes, I. O'Muircheartaigh and J. J. Gilmartin, *Eur Respir J*, 1997, **10**, 2535-2538.
10. W. Ebert, H. Dienemann, A. Fateh-Moghadam, M. Scheulen, N. Konietzko, T. Schleich and E. Bombardieri, *Eur J Clin Chem Clin Biochem*, 1994, **32**, 189-199.
11. R. Molina, X. Filella, J. M. Auge, R. Fuentes, I. Bover, J. Rifa, V. Moreno, E. Canals, N. Vinolas, A. Marquez, E. Barreiro, J. Borras and P. Viladiu, *Tumour Biol*, 2003, **24**, 209-218.
12. Z. H. Chen, Y. S. Wu, M. J. Chen, J. Y. Hou, Z. Q. Ren, D. Sun and T. C. Liu, *J Fluoresc*, 2013, **23**, 649-657.
13. J. Y. Hou, T. C. Liu, G. F. Lin, Z. X. Li, L. P. Zou, M. Li and Y. S. Wu, *Anal Chim Acta*, 2012, **734**, 93-98.
14. A. He, T. C. Liu, Z. N. Dong, Z. Q. Ren, J. Y. Hou, M. Li and Y. S. Wu, *J Clin Lab Anal*, 2013, **27**, 277-283.
15. Q. Yu, X. Zhan, K. Liu, H. Lv and Y. Duan, *Anal Chem*, 2013, **85**, 4578-4585.

16. L. P. Zhong, H. G. Zhu, C. P. Zhang, W. T. Chen and Z. Y. Zhang, *Int J Oral Maxillofac Surg*, 2007, **36**, 230-234.
17. L. Zhu, L. Xu, N. Jia, B. Huang, L. Tan, S. Yang and S. Yao, *Talanta*, 2013, **116**, 809-815.
18. T. Lovgren, I. Hemmila, K. Pettersson, J. U. Eskola and E. Bertoft, *Talanta*, 1984, **31**, 909-916.
19. L. J. Kricka, *Clin Chem*, 1994, **40**, 347-357.
20. T. Myyrylainen, S. M. Talha, S. Swaminathan, R. Vainionpaa, T. Soukka, N. Khanna and K. Pettersson, *J Nanobiotechnology*, 2010, **8**, 27.
21. G. F. Lin, T. C. Liu, L. P. Zou, J. Y. Hou and Y. S. Wu, *Luminescence*, 2013, **28**, 401-406.
22. A. M. Gutierrez, J. J. Ceron, B. A. Marsilla, M. D. Parra and S. Martinez-Subiela, *Can J Vet Res*, 2012, **76**, 136-142.
23. B. Huang, H. Xiao, J. Zhang, L. Zhang, H. Yang, Y. Zhang and J. Jin, *Arch Toxicol*, 2009, **83**, 619-624.
24. H. Kimura, M. Mukaida, G. Wang, J. Yuan and K. Matsumoto, *Forensic Sci Int*, 2000, **113**, 345-351.
25. K. Matsumoto, J. Yuan, G. Wang and H. Kimura, *Anal Biochem*, 1999, **276**, 81-87.
26. Z. Q. Ren, T. C. Liu, J. Y. Hou, M. J. Chen, Z. H. Chen, G. F. Lin and Y. S. Wu, *Luminescence*, 2013.
27. J. W. Findlay, W. C. Smith, J. W. Lee, G. D. Nordblom, I. Das, B. S. DeSilva, M. N. Khan and R. R. Bowsher, *J Pharm Biomed Anal*, 2000, **21**, 1249-1273.
28. G. Lin, H. Huang, T. Liu, C. He, J. Liu, S. Chen, J. Hou, Z. Ren, W. Dong and Y. Wu, *J Virol Methods*, 2014, **206**, 89-94.
29. P. E. De Pauw, I. Vermeulen, O. C. Ubani, I. Truyen, E. M. Vekens, F. T. van Genderen, J. W. De Grijse, D. G. Pipeleers, C. Van Schravendijk and F. K. Gorus, *Clin Chem*, 2008, **54**, 1990-1998.
30. C. Blake, M. N. Al-Bassam, B. J. Gould, V. Marks, J. W. Bridges and C. Riley, *Clin Chem*, 1982, **28**, 1469-1473.
31. K. J. Dean, S. G. Thompson, J. F. Burd and R. T. Buckler, *Clin Chem*, 1983, **29**, 1051-1056.
32. I. Hemmila, V. M. Mukkala, M. Latva and P. Kiilholma, *J Biochem Biophys Methods*, 1993, **26**, 283-290.

33. T. Tokairin, Y. Nishikawa, Y. Doi, H. Watanabe, T. Yoshioka, M. Su, Y. Omori and K. Enomoto, *J Hepatol*, 2002, **36**, 725-733.

34. M. Careri, L. Elviri, J. B. Lagos, A. Mangia, F. Speroni and M. Terenghi, *J Chromatogr A*, 2008, **1206**, 89-94.

35. X. Wang, Q. Y. Zhang, Z. J. Li, X. T. Ying and J. M. Lin, *Clin Chim Acta*, 2008, **393**, 90-94.

36. J. Y. Lin and Y. C. Chen, *Talanta*, 2011, **86**, 200-207.

Tables Captions

Table 1 Analytical recovery of CYFRA 21-1 and CEA added to serum samples.

Table 2 Precision of our novel assay.

Table 3 Dilution Linearity of our novel assay for CYFRA 21-1 and CEA.

Table 1

Analytical recovery of CYFRA 21-1 and CEA added to serum samples.

Sample	CYFRA 21-1 (ng/mL)			Sample	CEA (ng/mL)		
(ng/mL)	Expected	Observed	Recovery	(ng/mL)	Expected	Observed	Recovery
21.6	100	101.5	101.5%	15.7	100	103.8	103.8%
	200	197.6	98.8%		200	197.2	98.6%
	400	421.6	105.4%		400	410.9	102.7%
30.1	100	98.6	98.6%	29.3	100	101.5	101.5%
	200	210.2	105.1%		200	209.7	104.9%
	400	405.9	101.5%		400	386.7	96.7%
62.3	100	98.7	98.7%	33.8	100	97.3	97.3%
	200	196.3	98.2%		200	208.4	104.2%
	400	418.4	104.6%		400	378.1	94.5%

CEA, carcinoembryonic antigen; CYFRA 21-1, cytokeratin 19 fragment.

Table 2

Precision of our novel assay.

	Sample	CYFRA 21-1 (ng/mL)			Sample	CEA (ng/mL)		
		Mean	SD	CV		Mean	SD	CV
Within-run (n=12)	1	17.3	0.67	3.9%	1	9.81	0.46	4.7%
	2	45.9	2.82	6.2%	2	69.1	1.73	2.5%
	3	82.5	4.05	4.9%	3	75.6	3.33	4.4%
Between-run (n=15)	1	18.1	1.03	5.6%	1	10.3	0.58	5.6%
	2	47.3	3.14	6.6%	2	67.2	2.58	3.8%
	3	84.2	5.83	6.9%	3	78.7	5.19	6.5%

CV, coefficient of variation; SD, standard deviation; CEA, carcinoembryonic antigen; CYFRA 21-1, cytokeratin 19 fragment.

Table 3

Dilution Linearity of our novel assay for CYFRA 21-1 and CEA.

Sample	Dilution	CYFRA 21-1 (ng/mL)			CEA (ng/mL)		
		Expected	Observed	Recovery	Expected	Observed	Recovery
1	NA		39.2			40.8	
	1:2	19.6	20.1	102.6%	20.4	20.9	102.5%
	1:4	9.80	9.65	98.5%	10.2	9.72	95.2%
	1:8	4.90	4.98	101.6%	5.10	4.89	95.8%
	1:16	2.45	2.55	104.1%	2.55	2.45	96.1%
2	NA		80.7			110.5	
	1:2	40.4	39.5	97.8%	55.3	56.1	101.4%
	1:4	20.2	21.1	104.5%	27.6	26.9	97.4%
	1:8	10.1	9.8	97.0%	13.8	14.1	102.2%
	1:16	5.05	5.12	101.4%	6.90	6.67	96.6%
3	NA		146.8			230.7	
	1:2	73.4	73.9	100.7%	115.4	116.8	101.2%
	1:4	36.7	37.3	101.6%	57.7	58.1	100.7%
	1:8	18.4	17.9	97.3%	28.8	28.1	97.6%
	1:16	9.18	9.32	101.5%	14.4	13.9	96.5%

NA, not applicable; CEA, carcinoembryonic antigen; CYFRA 21-1, cytokeratin 19 fragment.

Figure Captions

Fig. 1. Example of a magnetic nanoparticle-based dual-label TRFIA employing europium and samarium chelate labels for simultaneous determination of CYFRA 21-1 and CEA.

Fig. 2. Standard curves and intra-assay precision profile of our novel assay for CYFRA 21-1 and CEA. Each point was based on 10 replicates.

Fig. 3. High-dose signal saturation (hook-effect) of our novel assay for CYFRA 21-1 and CEA.

Fig. 4. Total error was plotted as the mean bias (M) ± the 90% confidence limits of imprecision (U, L), and the LLOQs for CYFRA 21-1 (A) and CEA (B) were defined as the concentrations where RE was 25%.

Fig. 5. Graphical comparisons of the present TRFIA and CLIA results for determination of CYFRA 21-1 (A) and CEA (B).

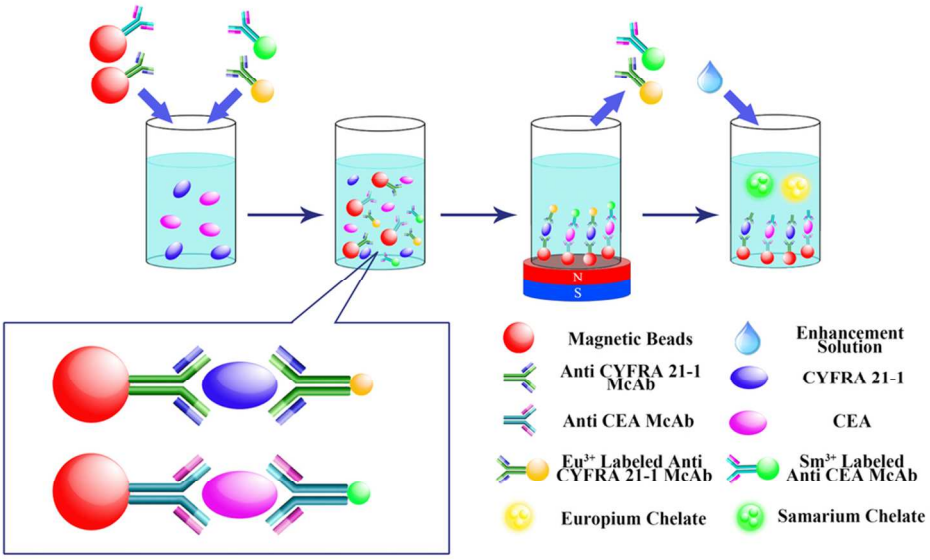

Fig. 1. Example of a magnetic nanoparticle-based dual-label TRFIA employing europium and samarium chelate labels for simultaneous determination of CYFRA 21-1 and CEA.
93x56mm (300 x 300 DPI)

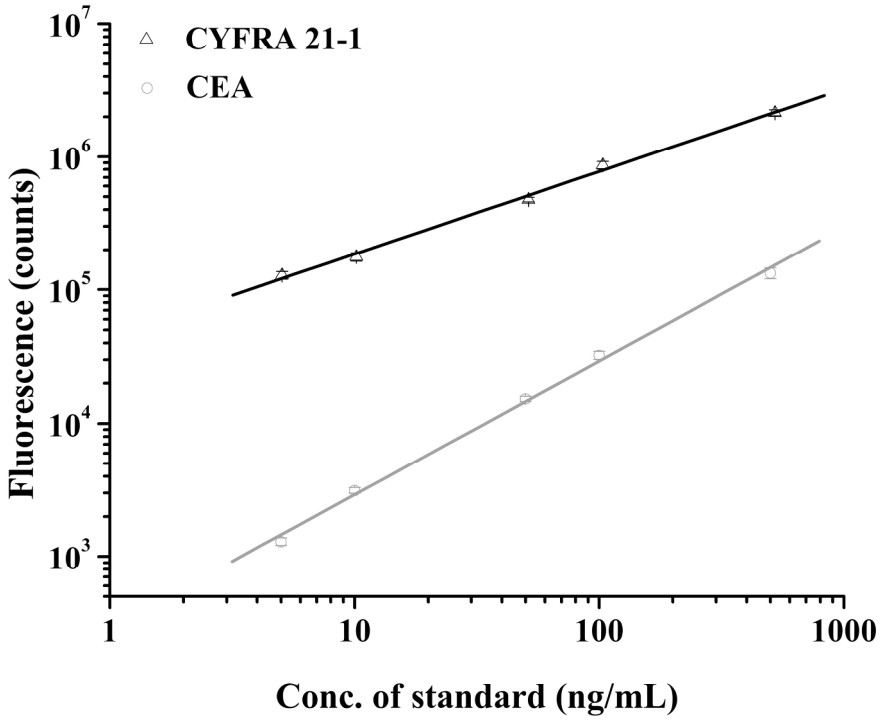

Fig. 2. Standard curves and intra-assay precision profile of our novel assay for CYFRA 21-1 and CEA. Each point was based on 10 replicates.
211x176mm (300 x 300 DPI)

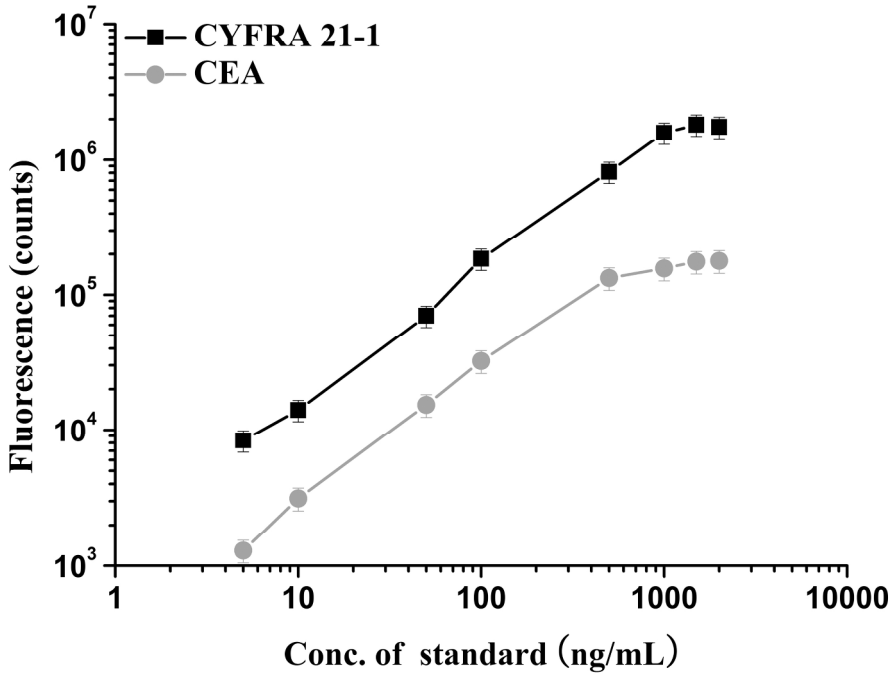

Fig. 3. High-dose signal saturation (hook-effect) of our novel assay for CYFRA 21-1 and CEA.
211x165mm (300 x 300 DPI)

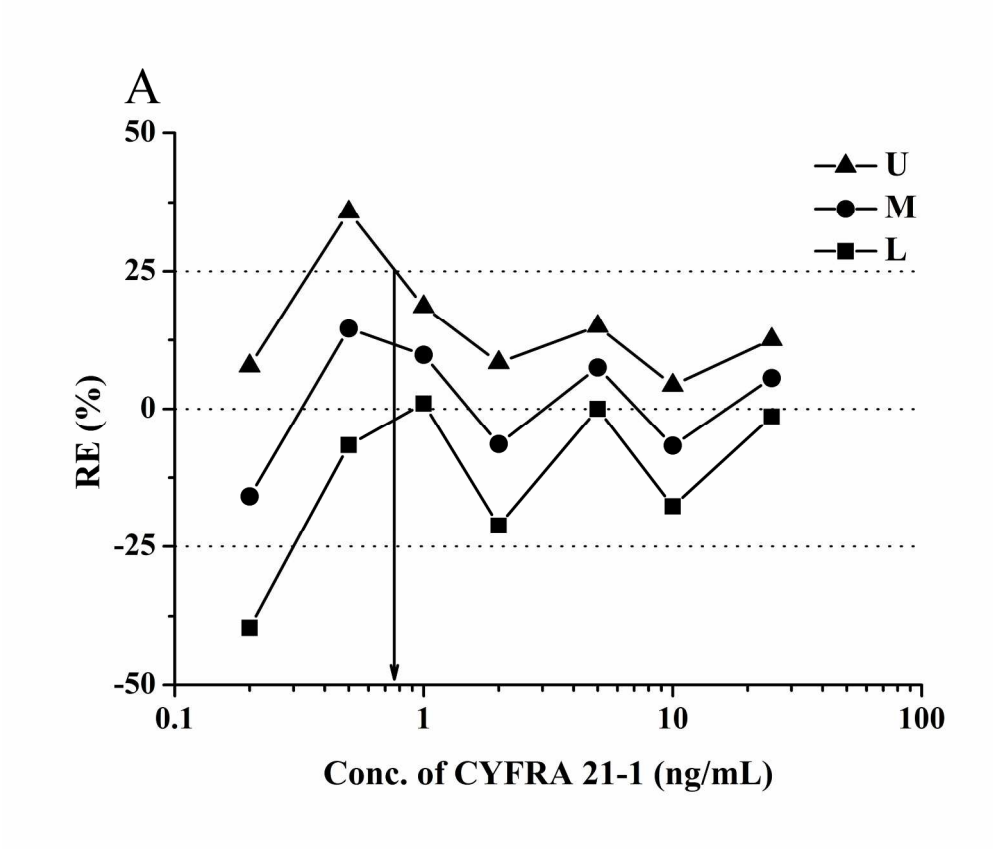

Fig. 4. Total error was plotted as the mean bias (M) the 90% confidence limits of imprecision (U, L), and the LLOQs for CYFRA 21-1 (A) and CEA (B) were defined as the concentrations where RE was 25%.
224x190mm (300 x 300 DPI)

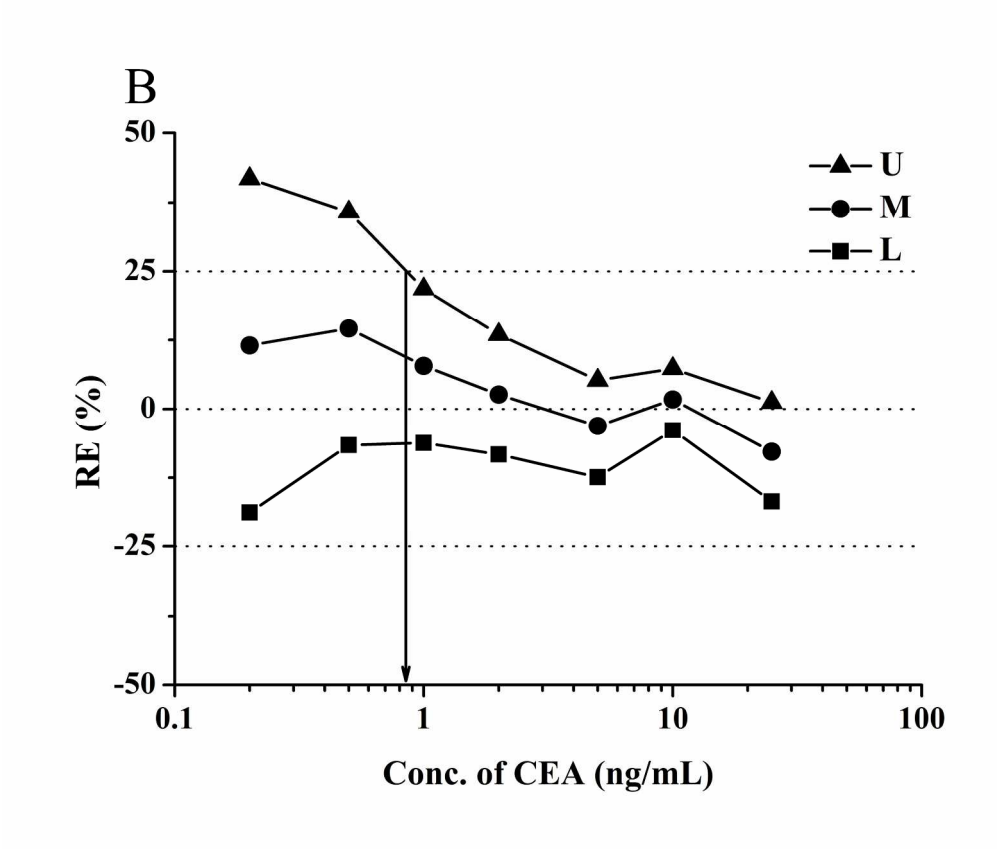

Fig. 4. Total error was plotted as the mean bias (M) the 90% confidence limits of imprecision (U, L), and the LLOQs for CYFRA 21-1 (A) and CEA (B) were defined as the concentrations where RE was 25%.
224x190mm (300 x 300 DPI)

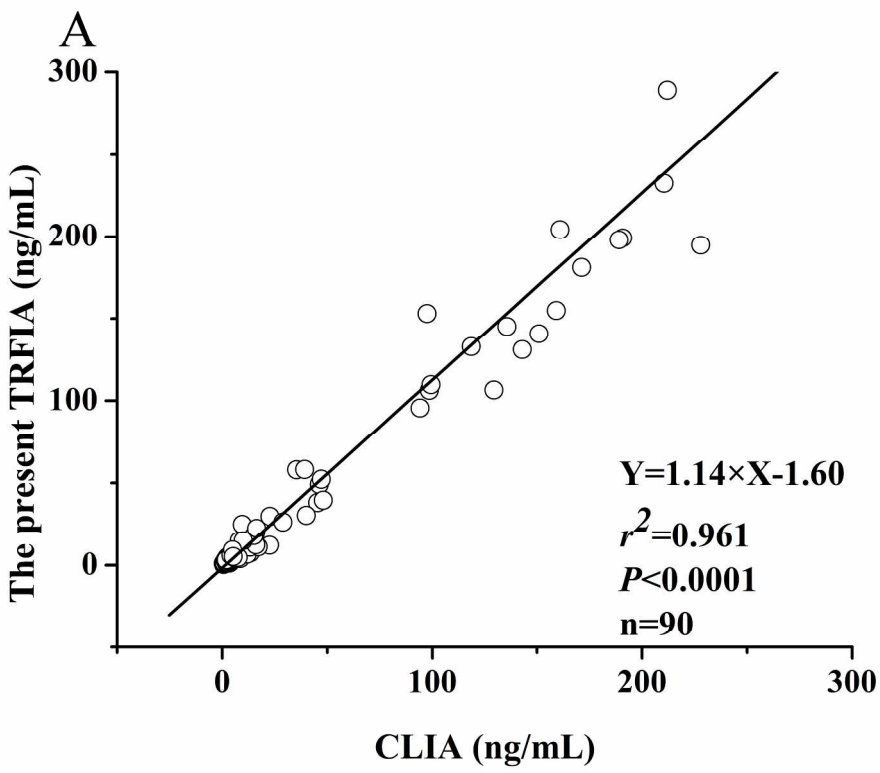

Fig. 5. Graphical comparisons of the present TRFIA and CLIA results for determination of CYFRA 21-1 (A) and CEA (B).
223x197mm (300 x 300 DPI)

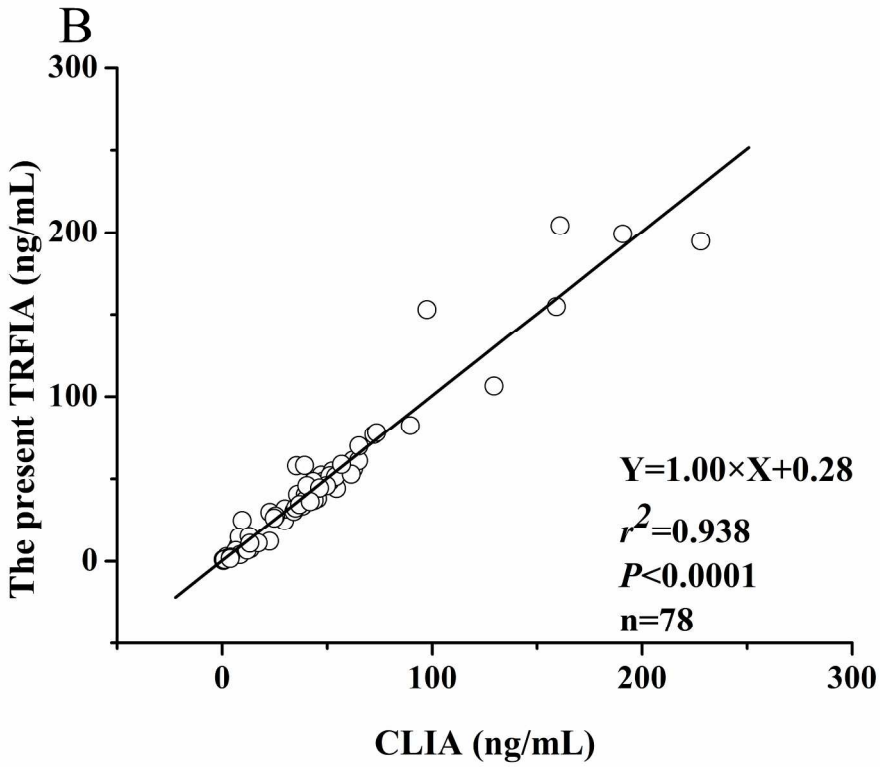

Fig. 5. Graphical comparisons of the present TRFIA and CLIA results for determination of CYFRA 21-1 (A) and CEA (B).
223x197mm (300 x 300 DPI)